Observation of Resolved Glucose Signals in ^{1}H NMR Spectra of the Human Brain at 4 Tesla

Rolf Gruetter, Michael Garwood, Kâmil Uğurbil, Elizabeth R. Seaquist

Measurement of the resonances of glucose between 3.2 and 3.9 ppm in ^{1}H NMR spectra from the human brain is difficult due to spectral overlap with peaks from more concentrated metabolites. The H1 resonance of α-D-glucose at 5.23 ppm is resolved from other metabolite peaks, but potentially overlaps with the intense water signal at 4.72 ppm. This paper demonstrates that the increased resolution at 4 Tesla permits to suppress the water signal sufficiently to reliably detect glucose directly at 5.23 ppm by ^{1}H MRS and the estimated peak intensity is consistent with previous ^{13}C NMR quantification.

Key words: glucose; brain; human; *in vivo* ^{1}H NMR.

INTRODUCTION

Glucose metabolism is essential for normal brain function and it is well established that a continuous supply of glucose from blood is necessary for normal cerebral metabolism (1, 2). The main route of glucose transport into the brain cell is across the blood-brain barrier (3, 4), which occurs by facilitated diffusion (5) mediated by specific transporter molecules (6). Glucose transport has been suggested to increase in chronic hypoglycemia and seizures and to decrease in chronic hyperglycemia and Alzheimer's disease (7–9). The size of the intracerebral glucose pool is an important indicator whether glucose transport at the blood-brain barrier is rate-limiting for cell metabolism, since the K_m of hexokinase is very low. Cerebral glucose has been measured in animal brain by rapid tissue extraction (10) which may suffer from artifacts due to agonal cerebral glucose metabolism. However, rapid tissue extraction is a method not applicable to humans. Noninvasive methods based on the administration of radiotracer methods have been used to study cerebral glucose metabolism (e.g., 11). However, radiotracer methods do not permit direct measurement of brain glucose content. The radiolabel enters the brain either as non-metabolizable glucose analogs (12) or labeled glucose (13). In the latter case, the potential label accumulation in more concentrated metabolites such as glutamate and glutamine (14) can obscure the signal from tissue glucose.

Despite its importance for neurophysiology, the direct measurement of brain glucose content has not been available until recently, when NMR was used. Resolved glucose signals can be observed in ^{13}C NMR spectra from the mammalian head (15, 16), and the potential of NMR to quantify glucose concentrations was demonstrated recently by Mason *et al.* (17). This elegant quantification method relied upon postmortem analysis of rat brain lactate and hence is not applicable to humans. The first quantification of glucose in the human brain was performed by ^{13}C NMR using intravenous infusions of [1-^{13}C]-D-glucose (18). In this study, when the plasma glucose was at euglycemia (i.e., a plasma glucose concentration of 4.8 m*M*) brain glucose content was determined to be 1 μmol/g.

Evidence that glucose signals might contribute to the ^{1}H NMR spectrum was provided by the observation of increased signal intensities at 3.4 ppm at 1.5–2 Tesla observed in hypoglycemic patients with Type 1 diabetes (19). However, the assignment of this peak is complicated by overlap with signals from *myo*-inositol and taurine (20). Although quantification of the glucose peak at 3.44 ppm has been attempted (21, 22), the reliability of these results has been unsatisfactory despite the use of more advanced fitting procedures (23). To eliminate the overlapping resonances, a more cautious approach early proposed to use difference spectra during glucose infusions (24).

Glucose has a single, well resolved resonance at 5.23 ppm from the H1 of α-D-glucose. Attempts to detect this resonance reliably have been only successful during hyperglycemia when using heteronuclear multiple quantum methods in conjunction with strong gradients and ^{13}C glucose infusions in animal brain studies (25, 26). Direct detection of this peak has not been reported, most likely due to its close proximity to the water peak at 4.72 ppm which corresponds to a frequency separation of 32 Hz at 1.5 Tesla from 5.23 ppm. In addition, the glucose intensity is expected to be weak: Given the 1 μmol/g brain glucose concentration at euglycemia (18) and the 60:40 anomeric equilibration ratio, this peak corresponds to 400 nmol/g single proton intensity, which is approximately 1% of the creatine (Cr) methyl peak at 3.03 ppm, neglecting contributions from macromolecules (27). However, at 4 Tesla the peak is 75 Hz from the water and

MRM 36:1–6 (1996)

From the Clinical Research Center and Center for MR Research, Departments of Medicine (E.R.S.) and Radiology (R.G., M.G., K.U.), University of Minnesota, Minneapolis, Minnesota.

Address correspondence to: Rolf Gruetter, Ph.D., Center for MR Research, Department of Radiology, Director, Clinical Research Center Satellite, University of Minnesota, 385 East River Road, Minneapolis, MN 55455.

Received December 12, 1995; revised February 15, 1996; accepted February 18, 1996.

This work was supported in part by grant RR07089, Biotechnological Research Resources Program, and in part by grant M01RR00400, General Clinical Research Center Program, National Center for Research Resources and by a grant from the Minnesota Medical Foundation MRF 107-95.

0740-3194/96 $3.00

the signal-to-noise ratio is significantly higher, which increases the potential of reducing water contributions to a low-order polynomial baseline at this chemical shift. This paper presents the direct observation of the 5.23 ppm glucose signal in localized ^{1}H NMR spectra of the human brain and an estimation of brain glucose concentration using the peak at 5.23 ppm. A preliminary report of part of this work has appeared as an abstract (28).

MATERIALS AND METHODS

Five subjects were studied after giving informed consent according to procedures approved by the Institutional Review Board. Subjects were placed on a cushion to minimize acoustic noise and wore ear plugs. Intravenous glucose infusions were performed either using a potentiation protocol (29), in which a fixed infusion rate of 600 ml/h of 10% weight/volume (Dextrose, Baxter Chemical Co.) was used, which raises plasma glucose to approximately 14 m*M* in normal subjects, or by using a variable-rate glucose infusion into the right antecubital vein, which was adjusted according to a modification of the glucose/insulin clamp technique (30). Samples for the determination of plasma glucose were obtained from a dorsal foot vein. Glucose infusions in this case were performed using a 50% weight/vol glucose solution (D50, Baxter Chemical Co.).

All experiments were performed on a 4 Tesla system (Siemens, Erlangen, Germany) with a SIS Co. Console using a 33-cm clear bore head gradient insert capable of switching 30 mT/m in 200 μs. Eddy current effects were assessed to be below 0.01% or 1 Hz at the isocenter (unpublished results).

During the study, subjects were supine on a quadrature surface coil consisting of an 18-cm diameter surface coil combined with a coplanar dual loop addition of equal diameter (31). The coil's sensitive volume was sufficient to detect signal from the posterior half of the human brain.

Localization was based on T_1 weighted images acquired in saggital and axial planes using the modified driven equilibrium Fourier transform (MDEFT) sequence (32). A 3 × 3 × 3 cm volume was selected in the occipital cortex centered at the midline to avoid blood vessels and the occipital ventricles.

The pulse sequence was initially based on a modification of the 3,0-DRY-STEAM version (33) of the stimulated echo spectroscopy (34, 35) or STEAM (36) using a repetition time (*TR*) of 3000 ms, echo time (*TE*) of 20 ms and a mixing time (TM) of 10 ms. To provide a narrow, reasonably B_1-sensitive excitation profile with a short overall pulse duration, water was suppressed using 25 ms Gaussian pulses. Three water suppression pulses were applied at the water resonance frequency before the first 90° slice selective excitation pulse, which was identical to the second and third 90° pulse used for localization, i.e., a 5-lobe sinc of 2 ms duration providing a 3-kHz bandwidth. The chemical shift displacement error was thus at most 0.25 cm for the glucose resonances. The bandwidth of the water suppression pulses was verified not to affect the glucose signal at 5.23 ppm using pulse simulations by solving the Bloch equations and phantom experiments using an aqueous solution of concentrated glucose (250 m*M* with 10 m*M* sodium acetate in 100 m*M* NaCl) placed in a 4-liter bottle. Crusher gradients in the *TE* periods and TM period were of 5 ms duration and 28 mT/m to suppress unwanted coherences and reduce potential signal from flowing blood. In a further improvement of the sequence, a fourth, identical water suppression pulse was added in the TM period (TM = 33 ms) corresponding to 3,1-DRYSTEAM (33) which provided an additional factor of 5–10 in water suppression.

Outer volume suppression was performed using a B_1-insensitive scheme (BISTRO, 37) in a plane parallel to the coil at the beginning of the pulse sequence applied just prior to the first three water suppression pulses.

Shimming is of critical importance to the elimination of unwanted water coherences at 5.23 ppm. Therefore, an automated shim sequence was used to adjust all first- and second-order shim coils based on the FASTMAP sequence (38) implemented as described in (39). This procedure resulted in water linewidths of 7–9 Hz and the linewidth for Cr was approximately 6–8 Hz.

Spectral processing consisted of zero-filling, exponential multiplication corresponding to 0–2 Hz line broadening and fast Fourier transform (FFT) using the spectrometer software (SIS Co., CA).

RESULTS AND DISCUSSION

Figure 1a shows sections of ^{1}H MR spectra obtained from the occipital region before (bottom) and during (middle and top) an intravenous glucose infusion (600 ml/h) during which the plasma glucose rose from euglycemia (approximately 5 m*M*) to hyperglycemia (approximately 14 m*M*, top). The spectra acquired at an intermediate level (middle trace) are also shown. Signal changes at 5.23 and 3.44 ppm are indicated by the arrows. The expansion of the corresponding spectral regions in Fig. 1b shows the rise of the resolved H1 peak at 5.23 ppm and also the change of the 3.44 ppm resonance. It is noteworthy that at 4 Tesla the latter peak is resolved from another distinct peak at 3.49 ppm, tentatively assigned to *myo*-inositol. In contrast, only one to two peaks are observed in the 3.3–3.5 ppm region at 1.5 and 2 Tesla. The extensive overlap present at this chemical shift, largely due to *myo*-inositol, has led to the acquisition of difference spectra at lower field strengths. The glucose signal was found to be less than 40% of the spectral amplitude at 3.44 ppm and much less so at 3.81 ppm (20, 40). The spectral changes that occur concurrently with glycemia and the stable, flat baseline at 4 Tesla confirm that the peak at 5.23 ppm is due to brain glucose. Figure 2 shows spectra acquired for 15 min at euglycemia (bottom) and for 6 min at hyperglycemia (approximately 30 m*M* plasma glucose, top) using the improved version of DRY-STEAM processed with 1 Hz linebroadening. The water intensity was suppressed to a level comparable to the intensity of the most prominent singlet peaks such as Cr, Cho, NAA. With this sequence, signal intensity from the glucose peak is clearly discernible at 5.23 ppm.

In order to assign this signal entirely to glucose, we used the previously established method of difference spectroscopy of glucose (20). The results of these measurements obtained from two different subjects are shown in Fig. 3. Figure 3a was acquired using the standard STEAM sequence (*TR* = 3000 ms, *TE* = 20 ms,

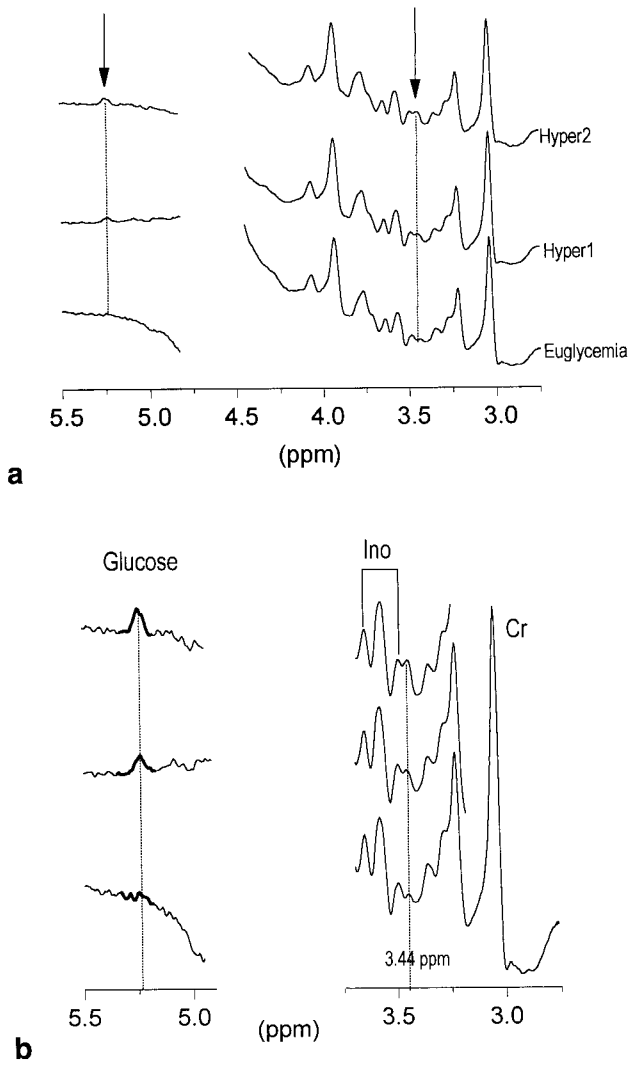

FIG. 1. Observation of specific signal changes in ^1H NMR spectra during intravenous glucose infusion. (a) The spectra were acquired during a fixed-rate intravenous glucose infusion (600 ml/h of 10% dextrose) during which plasma glucose rose from approximately 5 to 14 m*M* (29). Shown are spectra acquired before, during and at the end of the infusion study as serum glucose was elevated. The dotted lines indicate the most prominent signal changes at 5.23 and at 3.44 ppm. (b) Expansion of the spectra shown in (a) The region around the water resonance at 4.72 ppm has been deleted from this plot and the region around 3.44 ppm is enhanced by eliminating the trace distant to the 3.4 ppm region. Note that the peak at 3.44 ppm is resolved from a potential inositol resonance at 3.49 ppm identified by comparison with a *myo*-inositol phantom. Peak assignments are based on chemical shift and major constituent based on chemical analysis: Cr, creatine; Ino, inositol.

TM = 10 ms). Despite the presence of a strong residual water peak and concurrent baseline distortions, comparison of the *in vivo* difference spectrum with the phantom spectrum indicates similar relative chemical shifts and amplitudes which assign the difference to glucose as has been shown previously for the 3.44 ppm peak at 2.1 Tesla (20, 40). Using the STEAM sequence modified according to the 3,1-DRYSTEAM scheme (TM = 33 ms), we have been able to improve the water suppression considerably; the resulting *in vivo* difference spectrum and phantom spectrum from a different subject is shown in Fig. 3b. In this study, plasma glucose was raised to approximately 30 m*M*. It was thus possible to correlate more spectral features with the phantom spectrum. The dotted lines in Fig. 3b indicate the chemical shifts of the spectral features of glucose which are accurately present in the *in vivo* difference spectrum, thereby establishing (a) that the signal changes observed can be attributed almost entirely due to free glucose and (b) that the intensity of the 5.23 ppm peak correlates with the upfield glucose resonances. The *in vivo* spectrum in Fig. 3b also shows additional coherences around the water resonance which have variable phase and intensity. However, analysis of the time course showed that the signal at 5.23 ppm was unaffected by these coherences, as can also be seen in Fig. 5, which is from the same subject.

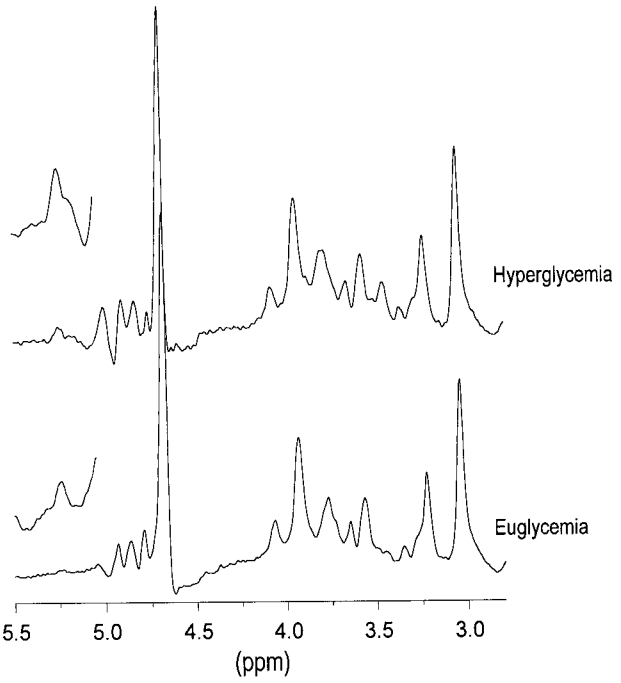

FIG. 2. ^1H NMR observation of brain glucose using DRYSTEAM. The bottom spectrum was obtained using 3,1-DRYSTEAM from a 15-min data accumulation during euglycemia and was processed with zero-filling prior to FFT. The top spectrum was acquired at approximately 30 m*M* plasma glucose over 6 min. The data is from the same subject as Fig. 3b. The downfield insets show the fivefold expanded region around 5.23 ppm processed with 4 Hz line broadening.

The stability of the peak at 5.23 ppm is shown by the time-resolved plot in Fig. 4, which indicates that the peak is readily observable at a 3-min time resolution. The baseline was corrected from 4.8–5.5 ppm based on fitting a second-order polynomial to the regions covering 4.8–5.1 ppm and 5.35–5.5 ppm. The stability of the resulting corrected baseline indicates that baseline correction with a second-order polynomial is a reliable method to remove residual water intensity at 5.23 ppm. The region from 4.8–5.5 ppm is expanded and overlaid in Fig. 4b to demonstrate the stability of the observation.

Phantom results (not shown) indicate that the modulation due to *J*-coupling is minor for short to moderately long echo times ($TE < 60$ ms) for both the peaks at 3.44

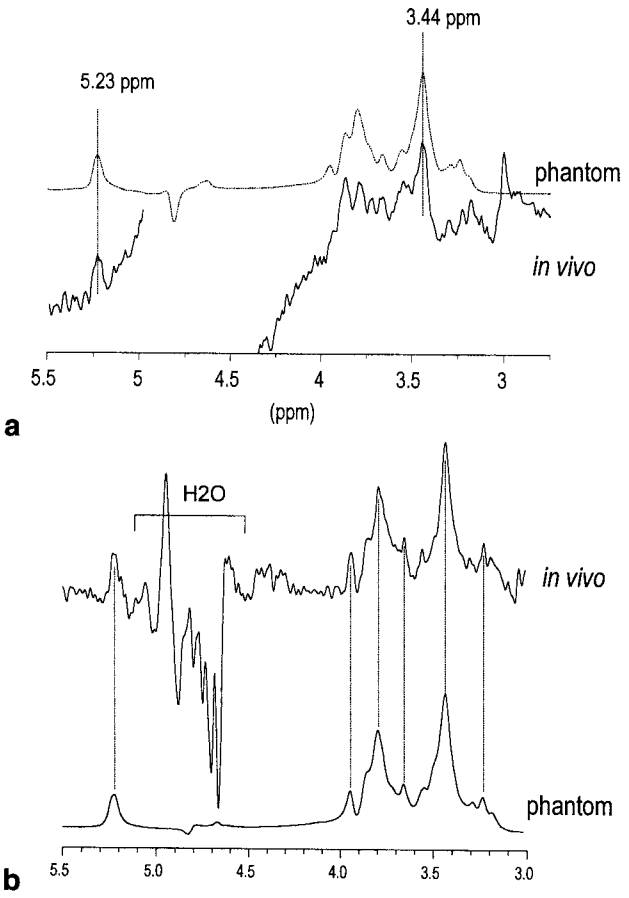

FIG. 3. Comparison of *in vivo* difference spectra with solution spectra. (a) The *in vivo* spectra were obtained from the same subject as in Fig. 1 by subtracting a spectrum acquired at euglycemia for 10 min from a spectrum acquired at approximately 14 m*M* for 15 min. Subtraction was performed with identical phase correction and by shifting the extensively zero-filled spectra in order to correct for field drift. The dotted vertical lines indicate the signal changes at 5.23 and at 3.44 ppm, which were observed at the same relative amplitudes and chemical shift as in the solution spectrum (dotted line). The solution spectrum was linebroadened to match singlet line widths in the *in vivo* spectrum. (b) The *in vivo* difference spectrum was obtained by subtracting a spectrum acquired at euglycemia from a spectrum acquired at approximately 30 m*M* plasma glucose concentration. The pulse sequence was an improved version of DRY-STEAM as described in the Methods section. Data processing was performed as in Fig. 1a. The dotted vertical lines indicate the chemical shifts characteristic for glucose at this field strength and *in vivo* linewidth. Comparison with the phantom spectrum (dotted line) shows that the in vivo spectrum corresponds almost entirely to the phantom spectrum, thereby assigning the majority of signal changes to free glucose.

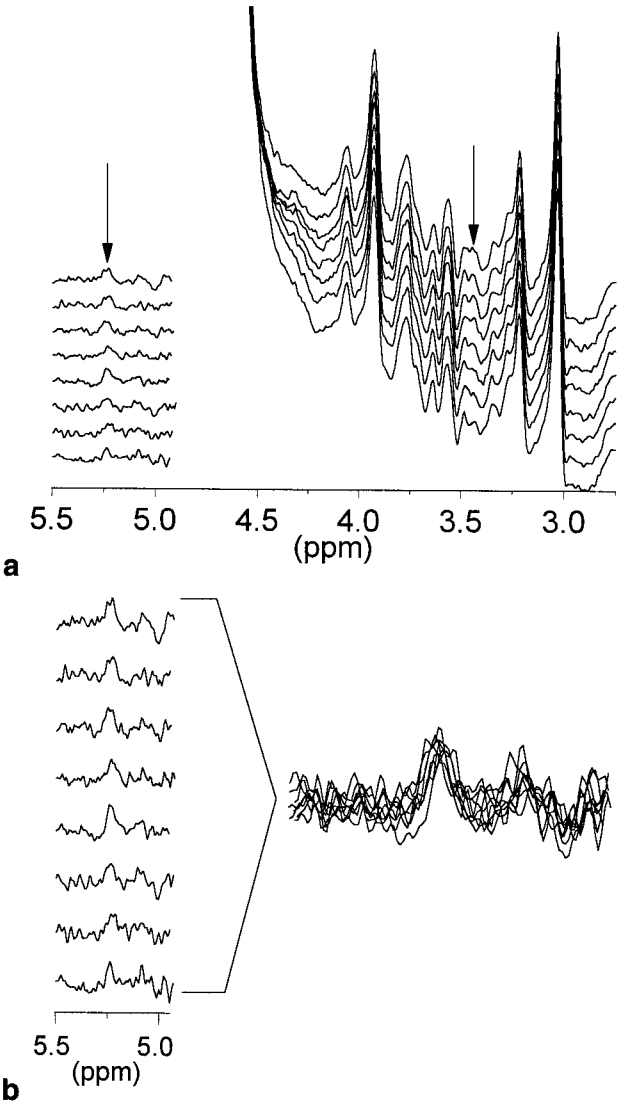

FIG. 4. Stability of the glucose observation. The spectra shown at a 3-min time resolution over a 30-min period demonstrate the stability of glucose observation despite the presence of the nearby intense water peak using 3,0-DRYSTEAM. The data are from the same subject as in Fig. 1. The arrows indicate the chemical shift at 5.23 and at 3.44 ppm. (a) In the downfield region, the baseline has been corrected by subtracting a second-order polynomial in the region from 4.8 to 5.5 ppm based on the baseline measured from 4.8–5.1 and from 5.3–5.5 ppm for each spectrum. (b) shows the downfield region of (a) more expanded in a stack plot as well as in an overlay which demonstrates the stability of the glucose measurements. Note that the variability of the glucose peak can be explained by noise, which is high due to the modest linebroadening of 1 Hz.

ppm and the peak at 5.23 ppm, which has a homonuclear coupling of 3.7 Hz. A series of echo times is shown in Fig. 5 which indicates a long T_2. Analysis of peak amplitudes for this measurement indicated a T_2 = 141 ms for the Cr methyl peak at 3.03 ppm and T_2 = 88 ms for the glucose peak at 5.23 ppm. In another subject, 8 echo times ranging from 20 to 270 ms were measured, which gave a T_2 for Cr of 130 ms. These values are consistent with the T_2 values reported by others for the methyl singlet peak of Cr for healthy human brain at 4 Tesla (41, 42) and indicate substantially long T_2 for glucose. The value of 88 ms is a lower bound for the actual T_2 of the H1 peak of glucose, because the glucose signal is decreased at longer echo times due to the homonuclear coupling of 3.7 Hz. The line width of this glucose peak is typically 2–3 Hz broader than that of the Cr peak. This increased linewidth can be explained by the unresolved doublet structure, and thus indicates similar T_2*. We therefore argue that T_2 is of the same order of magnitude as that of Cr.

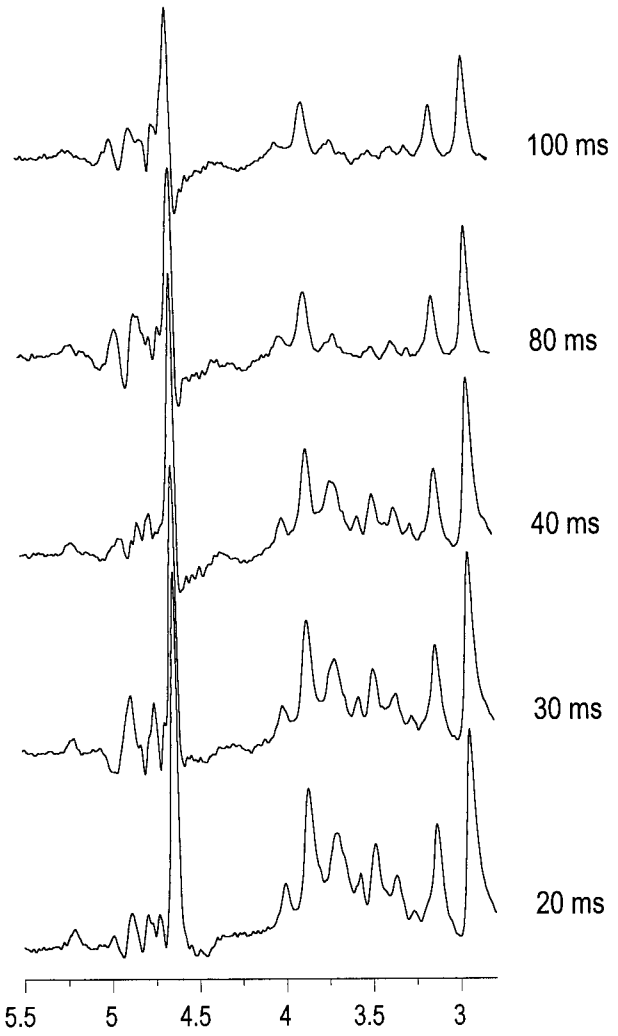

FIG. 5. Estimation of the T_2 of the glucose resonance. The stack plot shows a series of spectra acquired for 3 min at echo times TE = 20, 30, 40, 80, 100 ms. While all of the singlet methyl peaks (Cr, Cho, NAA) have T_2 in the range of 90–140 ms as determined from a fit of an exponential decay using nonlinear methods, the glucose T_2 was measured to be 88 ms, which represents an underestimation of the actual T_2 due to the homonuclear coupling of 3.7 Hz. The data is from the same subject as Figs. 2 and 3b.

Nevertheless, assuming that the T_2 of the glucose peak is identical to that of the Cr methyl peak, an overestimation of its actual T_2 by 50 ms would produce at most a 10% underestimation of the glucose signal at TE = 20 ms.

To estimate the cerebral glucose content, we have—as discussed above—assumed transverse relaxation effects of glucose and creatine to be the same. The concentration of creatine was assumed to be 10 mM, based on reported values by biopsy and ^1H MRS of the occipital region (43, 44). The peak intensities were determined by either plain integration from 5.14 to 5.34 ppm and from 2.93 to 3.07 ppm, respectively, or by peak fitting a Lorentzian peak simultaneously with a linear baseline at 5.23 ppm. Cr intensity was estimated by fitting two peaks at 3.04 ppm and at 2.96 ppm with a linear baseline using standard spectrometer software. The resulting *estimated* brain glucose concentrations are tabulated in Table 1. The values are consistent with the previous ^{13}C NMR quantification

TABLE 1
Brain Glucose Concentrations Estimated by ^1H NMR[a]

^1H NMR[b]	0.6	0.5	1.1	1.5	5.5	2.7
Plasma glucose (mM)	5.2	5.3	7.5	6.4	14.4	15.2

[a] Shown are values that cover the range of previously reported glycemias (18, 44).
[b] Brain glucose concentration was estimated by scaling the peak area at 5.23 ppm relative to 10 mM creatine methyl intensity at 3.03 ppm using a linear baseline correction.

(18, 45) which was performed by comparing the ^{13}C signal intensity to that of a phantom with concentrated glucose.

Further improvements in signal-to-noise ratio are possible by using two-fold more sensitive localization methods (46), such as ISIS (47) or PRESS (48) and by using smaller surface coils optimized for the anatomic region under investigation. These improvements should result in at least a threefold improved sensitivity over the current experiment.

CONCLUSIONS

The present paper demonstrates the feasibility of noninvasive quantification of the glucose proton NMR signal using the 5.23 ppm peak, which is a well resolved resonance at 4 Tesla. The signal-to-noise advantage of ^1H MRS permits to study smaller volumes without using ^{13}C enrichment thereby simplifying experimental design and expanding the potential usefulness of this measurement.

ACKNOWLEDGMENTS

The authors thank the staff of the Clinical Research Center, especially Dixie Lewis and Celeste Burckhardt, for support.

REFERENCES

1. W. M. Pardridge, Brain metabolism: a perspective from the blood-brain barrier. *Physiol. Rev.* **63,** 1481–1535 (1983).
2. M. E. Raichle, Circulatory and metabolic correlates of brain function in normal humans, *in* "Handbook of Physiology—The Nervous System V," Williams & Wilkins, Baltimore, pp. 643–674, 1983.
3. H. Lund-Andersen, Transport of glucose from blood to brain. *Physiol. Rev.* **59,** 305–352 (1979).
4. A. Gjedde, Blood-brain glucose transfer, *in* "Handbook of Experimental Pharmacology, vol. 103, Physiology and Pharmacology of the Blood-Brain" M. W. B. Bradbury, Ed.), pp. 65–117, Springer Verlag, New York, 1992.
5. A. Carruthers, Facilitated diffusion of glucose. *Physiol. Rev.* **70,** 1135–1176 (1990).
6. R. N. Kalaria, S. A. Gravina, J. W. Schmidley, G. Perry, S. I. Harik, The glucose transporter of the human brain and blood-brain barrier. *Ann. Neurol.* **24,** 757–764 (1988).
7. D. A. Pelligrino, J. C. LaManna, R. B. Duckrow, R. M. Bryan, S. I. Harik, Hyperglycemia and blood-brain barrier glucose transport. *J. Cereb. Blood Flow Metab.* **12,** 887–899 (1992).
8. R. N. Kalaria, S. I. Harik, Reduced glucose transporter at the blood-brain barrier and in cerebral cortex in Alzheimer's disease. *J. Neurochem.* **53,** 1083–1088 (1989).
9. D. C. DeVivo, R. R. Trifiletti, R. I. Jacobson, G. M. Ronen, R. A. Behmand, S. I. Harik, Defective glucose transport across the blood-brain barrier as a cause of persistent hypoglycorrhachia, seizures, and developmental delay. *N. Engl. J. Med.* **325,** 703–709 (1991).
10. J. E. Holden, K. Mori, G. A. Dienel, N. F. Cruz, T. Nelson, L. Sokoloff, Modeling the dependence of hexose distribution volumes in brain on plasma glucose concentration: implications for estimation of the local 2-deoxyglucose lumped constant. *J. Cereb. Blood Flow Metab.* **11,** 171–182 (1991).
11. J. L. Tyler, S. C. Strother, R. J. Zatorre, B. Alivisatos, K. J. Worsley, M. Diksic, Y. L. Yamamoto, Stability of regional cerebral glucose metab-

olism in the normal human brain measured by positron emission tomography. *J. Nucl. Med.* **29,** 631–642 (1988).
12. L. E. Feinendegen, H. Herzog, H. Wieler, D. D. Patton, A. Schmid, Glucose transport and utilization in the human brain: model using carbon-11 methylglucose and positron emission tomography. *J. Nucl. Med.* **27,** 1867–1877 (1986).
13. G. Blomqvist, A. Gjedde, M. Gutniak, V. Grill, L. Widén, S. Stone-Elander, E. Hellstrand, Facilitated transport of glucose from blood to brain in man and the effect of moderate hypoglycemia on cerebral glucose utilization. *Eur. J. Nucl. Med.* **18,** 834–837 (1991).
14. R. Gruetter, E. J. Novotny, S. D. Boulware, G. F. Mason, D. L. Rothman, J. W. Prichard, R. G. Shulman, Localized ^{13}C NMR spectroscopy in the human brain of amino acid labeling from D-[1-^{13}C] glucose. *J. Neurochem.* **63,** 1377–1385 (1994).
15. K. L. Behar, O. A. C. Petroff, J. W. Prichard, J. R. Alger, R. G. Shulman, Detection of metabolites in rabbit brain by ^{13}C NMR spectroscopy following administration of [1-^{13}C] glucose. *Magn. Reson. Med.* **3,** 911–920 (1986).
16. N. Beckmann, I. Turkalj, J. Seelig, U. Keller, ^{13}C NMR for the assessment of human brain glucose metabolism in vivo. *Biochemistry* **30,** 6362–6366 (1991).
17. G. F. Mason, K. L. Behar, D. L. Rothman, R. G. Shulman, NMR determination of intracerebral glucose concentration and transport kinetics in rat brain. *J. Cereb. Blood Flow Metabol.* **12,** 448–455 (1992).
18. R. Gruetter, E. J. Novotny, S. D. Boulware, D. L. Rothman, G. F. Mason, G. I. Shulman, R. G. Shulman, W. V. Tamborlane, Direct measurement of brain glucose concentrations in humans by ^{13}C NMR spectroscopy. *Proc. Natl. Acad. Sci. USA* **89,** 1109–1112 (1992). Erratum appears in vol. **89,** 12208.
19. T. Michaelis, K. D. Merboldt, W. Hänicke, M. L. Gyngell, J. Frahm, On the identification of cerebral metabolites in localized 1H NMR spectra of human brain in vivo. *NMR Biomed.* **5,** 90–98 (1991).
20. R. Gruetter, D. L. Rothman, E. J. Novotny, G. I. Shulman, J. W. Prichard, R. G. Shulman, Detection and assignment of the glucose signal in ^{1}H NMR difference spectra of the human brain. *Magn. Reson. Med.* **27,** 183–188 (1992).
21. R. Kreis, B. D. Ross, Cerebral metabolic disturbances in patients with subacute and chronic diabetes mellitus: detection with proton MR spectroscopy. *Radiology* **184,** 123–130 (1992).
22. K. D. Merboldt, H. Bruhn, W. Hänicke, T. Michaelis, J. Frahm, Decrease of glucose in the human visual cortex during photic stimulation. *Magn. Reson. Med.* **25,** 187–194 (1992).
23. S. W. Provencher, W. Hänicke, T. Michaelis, Automated quantitation of localized 1H MR spectra in vivo: capabilities and limitations, *in* "Proc., SMR, 3rd Annual Meeting, Nice, 1995," p. 1952.
24. R. Gruetter, D. L. Rothman, E. J. Novotny, G. I. Shulman, J. W. Prichard, R. G. Shulman, Detection of glucose by 1H NMR spectroscopy of the human brain during acute hyperglycemia, *in* "Proc., SMRM, 10th Annual Meeting, San Francisco, 1991," p. 1014.
25. P. C. M. van Zijl, A. S. Chesnick, D. DesPres, C. T. W. Moonen, J. Ruiz-Cabello, P. van Gelderen, *In vivo* proton spectroscopy and spectroscopic imaging of [1-^{13}C]-glucose and its metabolic products. *Magn. Reson. Med.* **30,** 544–551 (1993).
26. T. Inubushi, S. Morikawa, K. Kito, T. Arai, ^{1}H-detected in vivo ^{13}C NMR spectroscopy and imaging at 2T magnetic field: efficient monitoring of ^{13}C-labeled metabolites in the rat brain derived from 1-^{13}C-glucose. *Biochem. Biophys. Res. Commun.* **191,** 866–872 (1993).
27. K. L. Behar, D. L. Rothman, D. D. Spencer, O. A. C. Petroff, Analysis of macromolecule resonances in ^{1}H NMR spectra of human brain. *Magn. Reson. Med.* **32,** 294–302 (1994).
28. R. Gruetter, E. R. Seaquist, M. Garwood, K. Ugurbil, Observation of the 5.23 ppm resonance in ^{1}H NMR spectra of the human brain, *in* "Proc., SMR, 3rd Annual Meeting, Nice, 1995," p. 523.
29. E. R. Seaquist, R. P. Robertson, Effects of hemipancreatectomy on pancreatic alpha and beta cell function in healthy human donors. *J. Clin. Invest.* **89,** 1761–1766 (1992).
30. R. A. DeFronzo, J. D. Tobin, R. Andres, Glucose clamp technique: a method for quantifying insulin secretion and resistance. *Am. J. Physiol.* **237,** E214–223 (1979).
31. H. Merkle, M. Garwood, K. Ugurbil, Dedicated circularly polarized surface coil assembly for brain studies at 4T, *in* "Proc., SMRM, 12th Annual Meeting, New York, 1993," p. 1358.
32. J. H. Lee, M. Garwood, R. Menon, G. Adrianyi, P. Andersen, C. L. Truwit, K. Ugurbil, High contrast and fast three-dimensional imaging at high fields. *Magn. Reson. Med.* **34,** 308–312 (1995).
33. C. T. W. Moonen, P. C. M. van Zijl, Highly effective water suppression for in vivo proton NMR spectroscopy (DRYSTEAM). *J. Magn. Reson.* **88,** 28–41 (1990).
34. J. Granot, Selected volume excitation using stimulated echoes (VEST). Applications to spatially localized spectroscopy and imaging. *J. Magn. Reson.* **70,** 488–492 (1986).
35. R. Kimmich, D. Hoepfel, Volume-selective multipulse spin-echo spectroscopy. *J. Magn. Reson.* **72,** 379–384 (1987).
36. J. Frahm, K. D. Merboldt, W. Hänicke, Localized proton spectroscopy using stimulated echoes. *J. Magn. Reson.* **72,** 502–508 (1987).
37. Y. Luo, A. Tannus, M. Garwood, Frequency-selective elimination of coherent signal with B1 insensitivity: an improved outer volume suppression method (BISTRO), *in* "Proc., SMR, 3rd Annual Meeting, Nice, 1995," p. 1017.
38. R. Gruetter, Automatic, localized in vivo adjustment of all first- and second-order shim coils. *Magn. Reson. Med.* **29,** 804–811 (1993).
39. R. Gruetter, K. Ugurbil, A fast, automatic shimming technique by mapping along projections (FASTMAP) at 4 Tesla, *in* "Proc., SMR, 3rd Annual Meeting, Nice, 1995," p. 698.
40. R. Gruetter, E. J. Novotny, S. D. Boulware, D. L. Rothman, R. G. Shulman, ^{1}H NMR studies of glucose transport in the human brain. *J. Cereb. Blood Flow Metab.* **16,** 427–438 (1996).
41. S. Posse, C. A. Cuenod, R. Riesinger, D. LeBihan, R. S. Balaban, Anomalous transverse relaxation in ^{1}H spectroscopy in human brain at 4 Tesla. *Magn. Reson. Med.* **33,** 246–252 (1995).
42. G. F. Mason, J. W. Pan, S. L. Ponder, D. B. Twieg, G. M. Pohost, H. P. Hetherington, Detection of brain glutamate and glutamine in spectroscopic images at 4.1T. *Magn. Reson. Med.* **32,** 142–145 (1994).
43. O. A. C. Petroff, D. D. Spencer, J. R. Alger, J. W. Prichard, High-field proton magnetic resonance spectroscopy of human cerebrum obtained during surgery for epilepsy. *Neurology* **39,** 1197–1202 (1989).
44. J. Peeling, G. Sutherland, ^{1}H magnetic resonance spectroscopy of extracts of human epileptic neocortex and hippocampus. *Neurology* **43,** 589–594 (1993).
45. R. Gruetter, E. J. Novotny, S. D. Boulware, D. L. Rothman, G. F. Mason, G. I. Shulman, R. G. Shulman, W. V. Tamborlane, Non-invasive measurements of the cerebral steady-state glucose concentration and transport in humans by ^{13}C magnetic resonance, *in* "Frontiers in Cerebral Vascular Biology: Transport and its Regulation" (L. R. Drewes, A. L. Betz, eds.), *Adv. Exp. Med. Biol.* **331,** pp. 35–40, Plenum Press, New York (1993).
46. C. T. W. Moonen, M. von Kienlin, P. C. M. van Zijl, J. Cohen, J. Gillen, P. Daly, G. Wolf, Comparison of single-shot localization methods (STEAM and PRESS) for in vivo proton NMR spectroscopy. *NMR Biomed.* **2,** 201–208 (1989).
47. R. J. Ordidge, A. Connelly, J. A. B. Lohman, Image-selected in vivo spectroscopy (ISIS). A new technique for spatially selective NMR spectroscopy. *J. Magn. Reson.* **66,** 283–294 (1986).
48. R. J. Ordidge, M. R. Bendall, R. E. Gordon, A. Connelly, Volume selection for in-vivo biological spectroscopy, *in* "Magnetic Resonance in Biology and Medicine" (G. Govil, C. L. Khetrapal, A. Saran, Tata, eds.), McGraw-Hill, New Delhi, pp. 387–397, 1985.